Void-fraction and acoustic characteristics of gas bubbles entrained by a circular plunging jet

Richard Manasseh [a] *, **Hubert Chanson** [b]

[a]CSIRO Thermal & Fluids Engineering, PO Box 56, Highett, VIC 3190, Melbourne, Australia

[b]Department of Civil Engineering, University of Queensland, QLD 4072, Brisbane, Australia

Abstract

Void-fraction and acoustic measurements were made in circular plunging jets. Plunging jets efficiently dissolve gas in liquid, and are essential in many industrial and environmental systems. A resistivity probe measured both the void fraction and bubble count rate, which compared well with a solution of an advective diffusion equation. A hydrophone recorded sounds as bubbles were formed. Bubble-acoustic frequencies are inversely proportional to the cube root of bubble volume. The acoustic data were processed to extract both bubble count and bubble size data. The acoustic bubble count, accepting only realistic bubble pulses, was very similar to the resistivity probe counts. Use of the acoustic technique yielded new information on the bubble size distribution and on possible bubble breakup regimes. The results indicate an acoustic sensor would be useful in high void-fraction flows in industry or the environment, where more delicate probes would be impractical.

Keywords: Plunging jet; Bubble; Acoustic

1. Introduction

Plunging jet entrainment is a highly efficient mechanism for producing a gas-liquid interface. Applications include minerals-processing flotation cells, waste-water treatment, oxygenation of mammalian-cell bio-reactors, riverine re-oxygenation weirs and the understanding of plunging ocean breakers (e.g. Jameson 1995, Chanson 1997, Kolani et al. 1998).

Most studies into the air entrainment process of circular plunging jets have been qualitative (see reviews by Bin 1993 and Chanson 1997). It is well understood that plunging jet entrainment takes place when the jet impact velocity exceeds a critical velocity (e.g. Ervine et al. 1980, Cummings and Chanson 1999). Overall, the developing region of plunging jet flow is subjected to strong interactions between the entrained air bubbles and the momentum transfer mechanism (e.g. Chanson and Brattberg 1998).

*Corresponding author; E-mail: Richard.Manasseh@dbce.csiro.au

In the present study, intrusive probe measurements give flow properties like void fraction and bubble count rate, while the acoustic technique provides useful information on the bubble size distribution. Bubbles generate sounds upon formation and deformation (Minnaert 1933, Leighton 1994, Manasseh et al. 2000) and are responsible for most of the noise created by a plunging jet. Underwater acoustic sensors are made from robust piezoelectric crystals, and thus have the key advantage of being useful for practical measurements in the field or in industry where environments may be hostile.

This study aims to characterize both the bubbly flow properties and acoustic parameters in the developing flow region of a large plunging jet system. Intrusive resistivity probe data are complemented by acoustic details of the air-water flow. The acoustic technique was originally calibrated against precision laboratory photographs of individual bubbles (Manasseh 1997). In Manasseh et al. (2000) the acoustic technique was applied to a complex bubbly flow in a stirred tank, but comparisons with equivalent measurement techniques were limited. The present study takes further steps towards an acoustic signature technique for characterizing the performances of a bubbly flow system with large void fraction.

2. Experimental apparatus and methods

The experimental apparatus is shown in Fig. 1, which also defines some terms. It consists of a circular water jet issuing from a 0.025 m diameter nozzle, discharging vertically. The receiving channel is 0.3 m wide and 1.8 m deep with glass walls 10 mm thick. The nozzle is made of aluminium with a 1/2.16 contraction ratio designed with an elliptical profile. Upstream of the nozzle, water is supplied by a straight circular pipe (0.054 m internal diameter, 3.5 m long). The jet nozzle and pipe are vertical. The water supply (Brisbane tap water) comes from a constant-head tank with a water level about 12.9 m above the nozzle. The apparatus provides jet velocities between 0.3 and 7 m/s. The discharge was measured with an orifice meter (British Standards design) calibrated on-site with a volume-per-time technique. The error on the discharge measurement was less than 1%.

Measurements were taken on the jet diameter through the centreline. The displacement of the probes in the flow direction and direction normal to the jet support was controlled by two fine adjustment travelling mechanisms and measured with two Lucas Schaevitz Magnarules Plus MRU-012 and MRU-036. Overall the error in the probe position was less than 0.1 mm in each direction.

In the free-falling jet, clear water jet velocities and turbulent velocity fluctuations were measured using a Pitot tube and a conical hot-film probe system. The Pitot tube was connected to a Validyne pressure transducer scanned at 500 Hz. The hot-film used a special miniature probe (Dantec 55R42, 0.3 mm size) scanned at 40 kHz. It was initially calibrated with Pitot tube data. The velocity profiles were integrated and checked with the measured flow rate (within 2%) for jet velocities ranging from 1 to 5 m/s.

A single-tip resistivity probe (inner electrode 0.35 mm and outer electrode 1.42 mm) was used to measure void fraction and bubble count rates. The probe was excited by an air bubble detector (Ref. AS25240) with a response time less than 10 μs. Measurements were recorded with a scan rate of 5 kHz for 3 minutes.

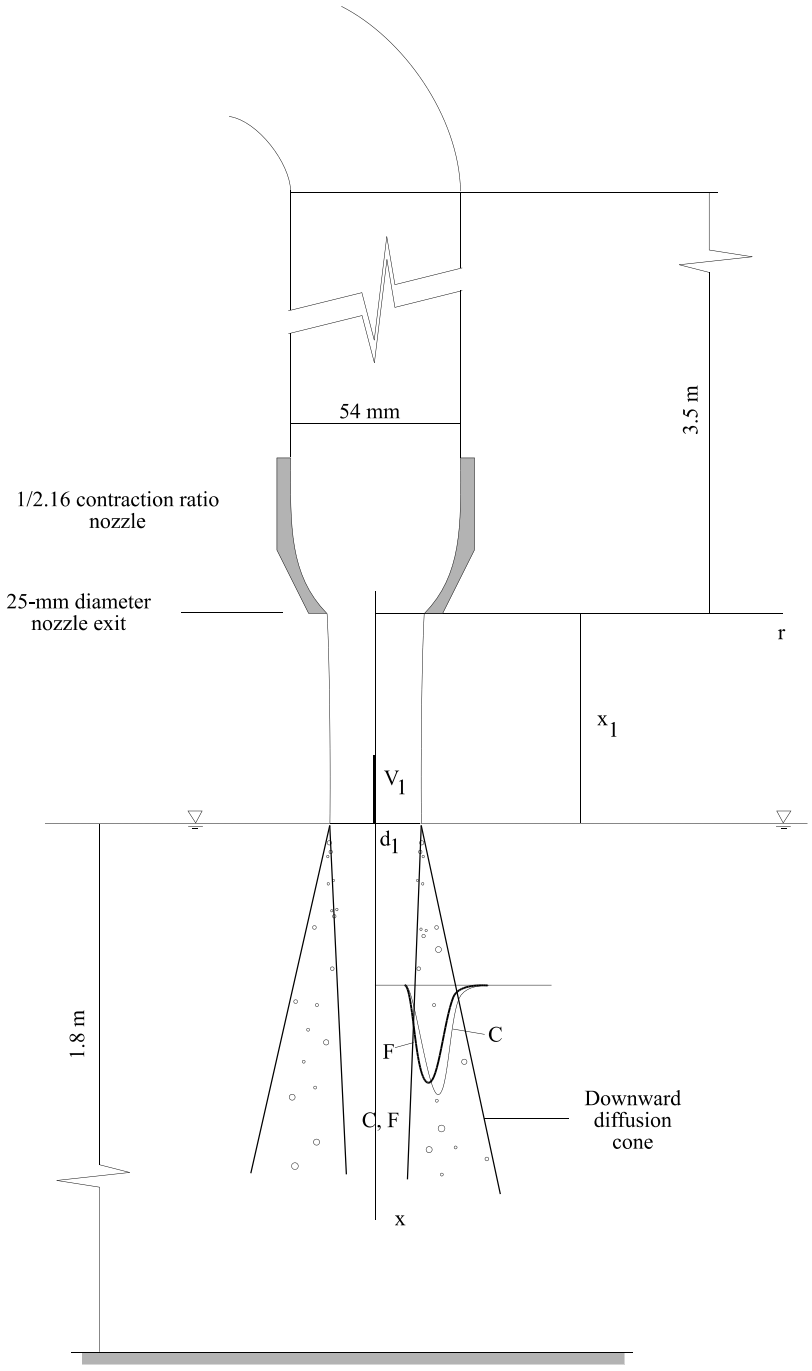

Figure 1. Vertical circular plunging jet apparatus

Underwater acoustics were measured with a hydrophone (Brüel and Kjær type 8103) connected to a Brüel and Kjær charge amplifier type 2635. A Digital Audio Tape (DAT) recorder (Sony TCD-D7) digitized the signal at 44.1 kHz, thereby implying an alias frequency around 22 kHz. The DAT recordings were processed with a HP35670A Dynamic Signal Analyzer. Fast Fourier Transforms (FFTs) were taken of each dataset being subsampled into 500 sets each 15.6 ms long to give a frequency span of 0-25.6 kHz. The same data were also processed by the bubble-acoustic software StreamTone running on a Pentium PC.

The error on the void fraction C was estimated as $\Delta C = 0.02$ for $0 \leq C$. The minimum detectable bubble chord length with resistivity probe methods is about 0.3 mm, and the minimum bubble size with the present acoustic analysis (see below) was also 0.3 mm. The accuracy of the clear-water velocity V was about $\Delta V/V = 1\%$. For the acoustic data, 95% confidence limits were calculated for the averaged spectrum for each run. At low speeds ($V_1 < 2.4$ m s^{-1} where V_1 is the mean velocity at jet impact), the acoustic signal was very intermittent. Although the representativity of these runs could not be checked, their averaged spectrum appeared statistically stationary within the 500 samples available. At higher speeds, bubble sound pulses come frequently, creating the characteristic 'rushing water' noise associated with a waterfall. Statistical stationarity is easily obtained within 500 samples, enabling representativity checks.

The free jet length could be varied by lowering the pool level up to 1 m below the nozzle. For each test, the water jet was extremely smooth and transparent; that is, no air entrainment was visible upstream of the impingement point. Velocity and velocity fluctuation distributions measured 5 mm downstream of the jet nozzle were uniform for nozzle velocities ranging from 0.5 to 5 m/s. In the present study, the free-jet lengths ranged from 0.005 up to 0.3 m, and the impingement velocities were between 0.5 and 6 m/s.

3. Distributions of void fraction and bubble count rate

Void fraction and bubble count rate data are presented in Fig. 2, for impact flow velocities V_1 of 3.9 m/s and 5.0 m/s and free-jet lengths of 0.005 m and 0.2 m respectively. Results for other velocities and free-jet lengths show similar curves. The void fraction measurements are compared with a simple analytical solution of the advective diffusion solution,

$$C = \frac{Q_{air}}{Q_w} \frac{1}{8D^{\#}X} \exp\left(-\frac{r_J^2+1}{8D^{\#}X}\right) I_0\left(\frac{r_J}{4D^{\#}X}\right) \quad (1)$$

where Q_{air} is the quantity of entrained air, Q_w is the water jet flow rate, $D^{\#} = 2D_t/(V_1 d_1)$, D_t is the advective diffusion coefficient, $X = (x - x_1)/d_1$, $R_J = 2r_J/d_1$, x is the distance along the flow direction (m) measured from the jet nozzle, r_J is the radial distance from the jet centreline, and I_0 is the modified Bessel function of the first kind of order zero, (Chanson 1997).

For each run, the values of Q_{air}/Q_w and $D^{\#}$ were determined from the best fit of the data to Eq. (1). Note that the data were best fitted by assuming $R_J = 2(r_J + dr_J)/d_1$

where $dr_J > 0$ increases with increasing X for a given experiment.

In the developing flow region, the void fraction distribution exhibits a peak ($C = C_{max}$) at $r_J = r_{JC_{max}}$. The distributions of bubble count rate F also show a maximum ($F = F_{max}$) in the developing flow region, but at $r_J = r_{JF_{max}}$, where $r_{JC_{max}}$ and $r_{JF_{max}}$ are significantly different. For $(x - x_1)/d_1 < 8$ and all jet lengths, the bubble count peak was consistently on the inside of the void-fraction peak: i.e., $r_{JC_{max}} < r_{JF_{max}}$. The result is consistent with the observations of Brattberg and Chanson (1998) for a plane jet.

4. Acoustic analysis and results

4.1. Acoustic spectrum

Acoustic spectra are shown in Fig. 3, for the same geometric conditions ($x_1 = 0.005$, $x - x_1 = 0.020$, $d_1 = 0.025$) as Fig. 2(a), and several impact velocities with identical free-jet lengths ($x_1 = 0.005$). Each spectrum was normalized to its integral and was shifted to account for the different amplification used during each experiment. In Fig. 3, the ordinate is a logarithmic scale and fine lines bracketing the central lines indicate the bounds of 95% statistical confidence intervals. High-velocity experiments show more acoustic energy illustrating that they are louder. Furthermore, each spectrum has a minimum in energy indicating that low-frequency noise (probably due to background turbulence, or possibly vibrations of swarms of bubbles as a whole) is below 400 Hz. At low jet velocities (e.g. V_1 = 3.11 m/s), individual bubble signals were clear and a broad peak was centred around f = 3.6 kHz. With increasing jet velocity, the frequency peak shifted to lower frequencies. For V_1 = 4.39 m/s, the peak was at about f = 1.7 kHz. Both characteristic frequencies are greater than the noise frequency and no high-pass filtering was required.

4.2. Bubble-size spectrum analysis

The relationship between bubble size and acoustic frequency is

$$f = \frac{1}{2\pi R_0}\sqrt{\frac{3\gamma P_\infty}{\rho}}, \tag{2}$$

where f is the frequency in Hz, P_∞ is the absolute liquid pressure, γ is the ratio of specific heats for the gas, ρ is the liquid density, and R_0 is the equilibrium bubble radius (Minnaert 1933). For this experiment Eq. (2) becomes

$$f = \frac{3.29}{R_0}. \tag{3}$$

An acoustic spectrum of frequencies f may be inverted to give a spectrum of bubble sizes R_0. However, it is not correct to simply plot the sound power spectrum against the reciprocal of frequency, as Eq. (2) would suggest. Larger bubbles are louder and therefore contribute more to the sound power. A spectral analysis would be biased unless a correction is introduced. Assumptions are required in comparing the relative excitation of bubbles. Pandit et al. (1992) proposed a simple treatment. The instantaneous sound pressure produced by a single bubble, $p(t)$, is given by

$$p(t)^2 = \frac{1}{f^2}\frac{3\gamma {P_\infty}^3/(4\pi^2\rho)}{(\gamma(\gamma-1)r)^2}X(t)^2, \tag{4}$$

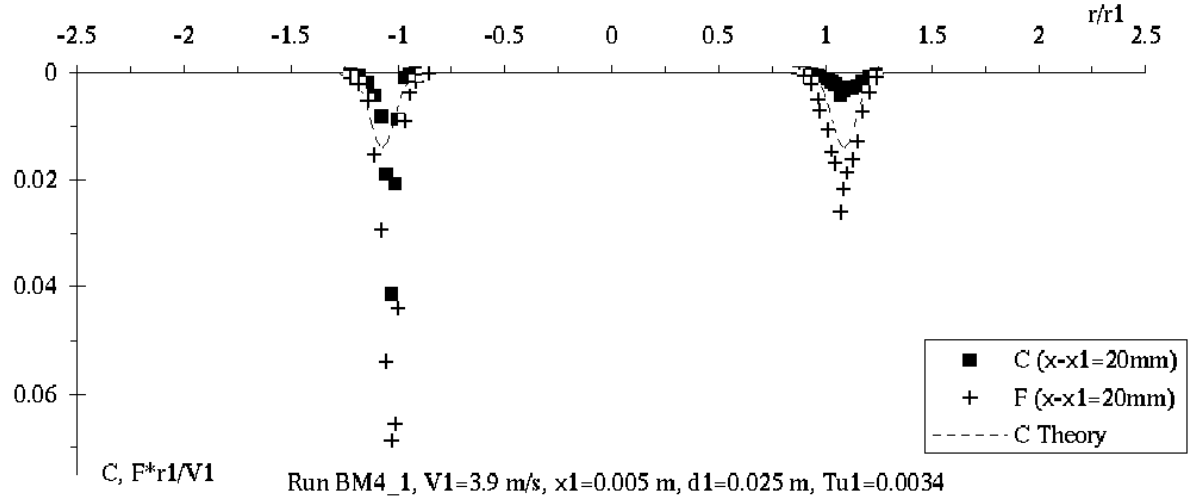

(a)

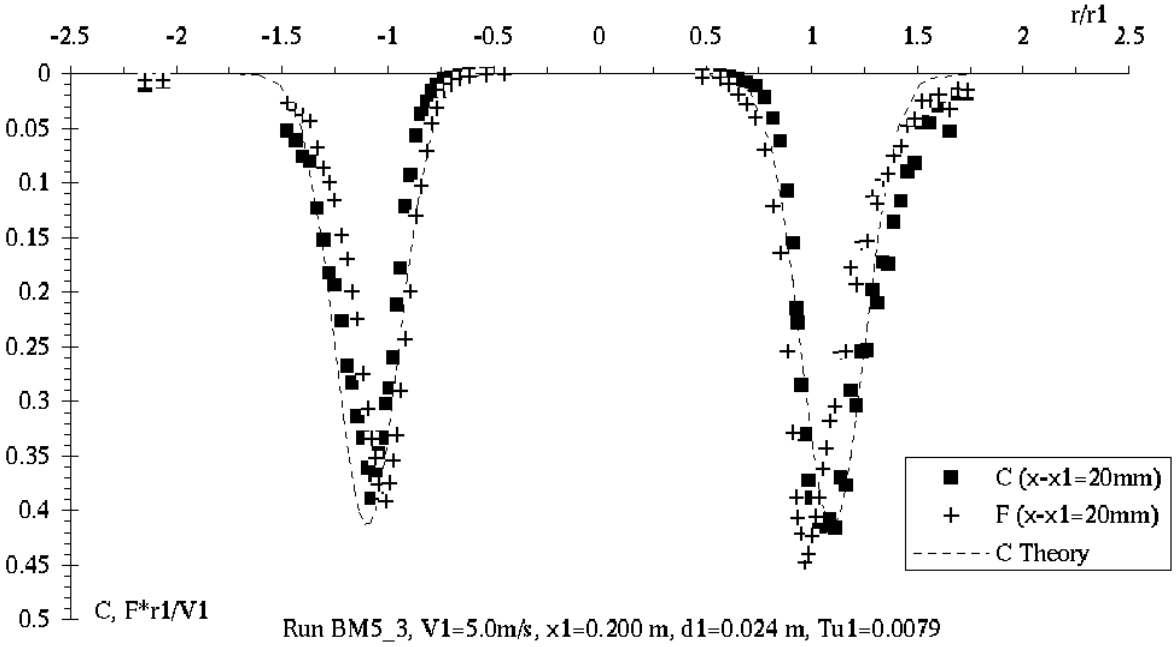

(b)

Figure 2. Void-fraction and bubble count, jet height 5 mm. (a): speed 3.9 m/s; (b) 5.0 m/s. Dashed line is solution of Eq. (1). Tu1 is turbulence intensity based on longitudinal velocity fluctuations.

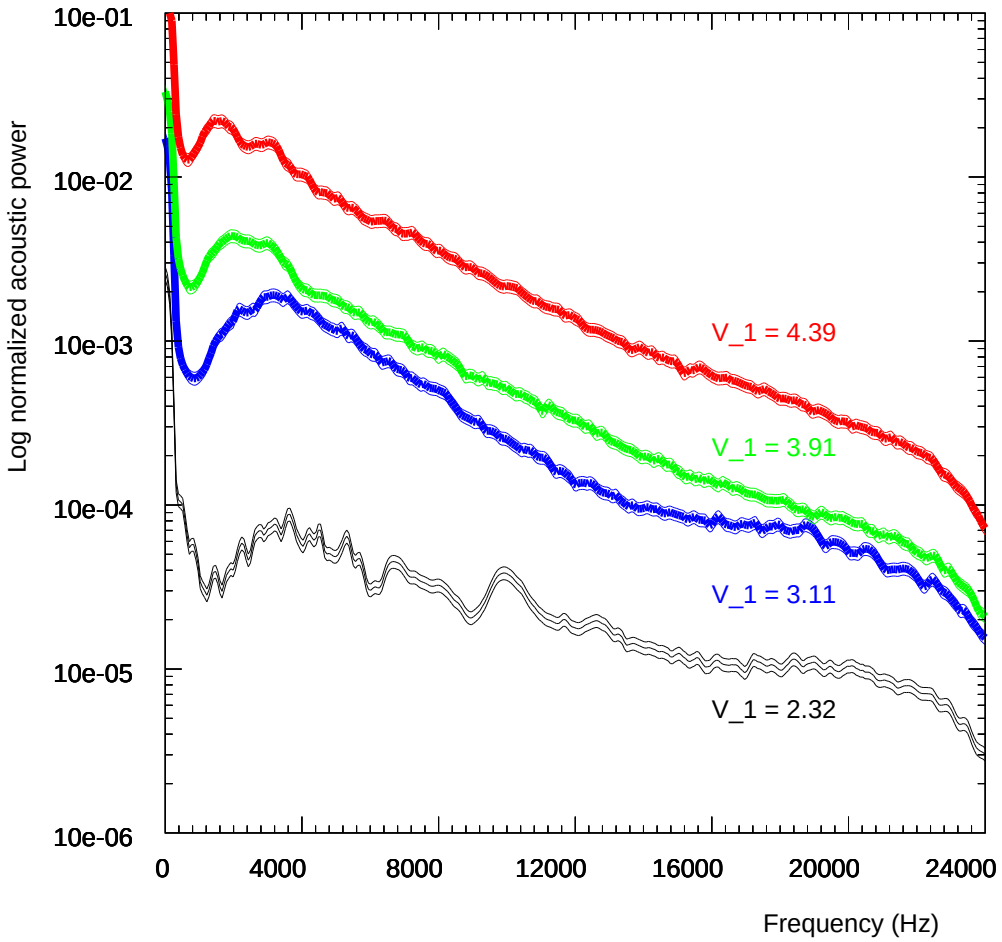

Figure 3. Acoustic spectra, jet height 5 mm

where r is the distance from the bubble and the time-dependent factor $X(t)$ is given by

$$X(t) = \left(\frac{4}{3} - \gamma\right)\left(\frac{R_0}{R(t)}\right)^{3\gamma-1} + \frac{1}{3}\left(\frac{R_0}{R(t)}\right)^2, \tag{5}$$

for adiabatic compression of the bubble, where $R(t)$ is the instantaneous bubble radius. For the simultaneous oscillations of n identical bubbles, the resultant summed sound pressure P, which would be measured by a hydrophone, is given by

$$P^2 = n\bar{p}^2, \tag{6}$$

where $\bar{p}$ is the RMS value of $p(t)$. This, using Eq. (4), yields the corrected value of the frequency spectrum, N, as

$$N = P^2 f^2 K, \tag{7}$$

where K is a function of the degree of excitation of the bubbles and of the distance between the bubbles and the hydrophone. Because sound power falls off as $1/r^2$, only bubbles

close to the hydrophone contribute to the measured sound. The degree of excitation of the bubbles ($R_0/\bar{R}$) might differ with bubble sizes. In a plunging jet flow, it is likely that

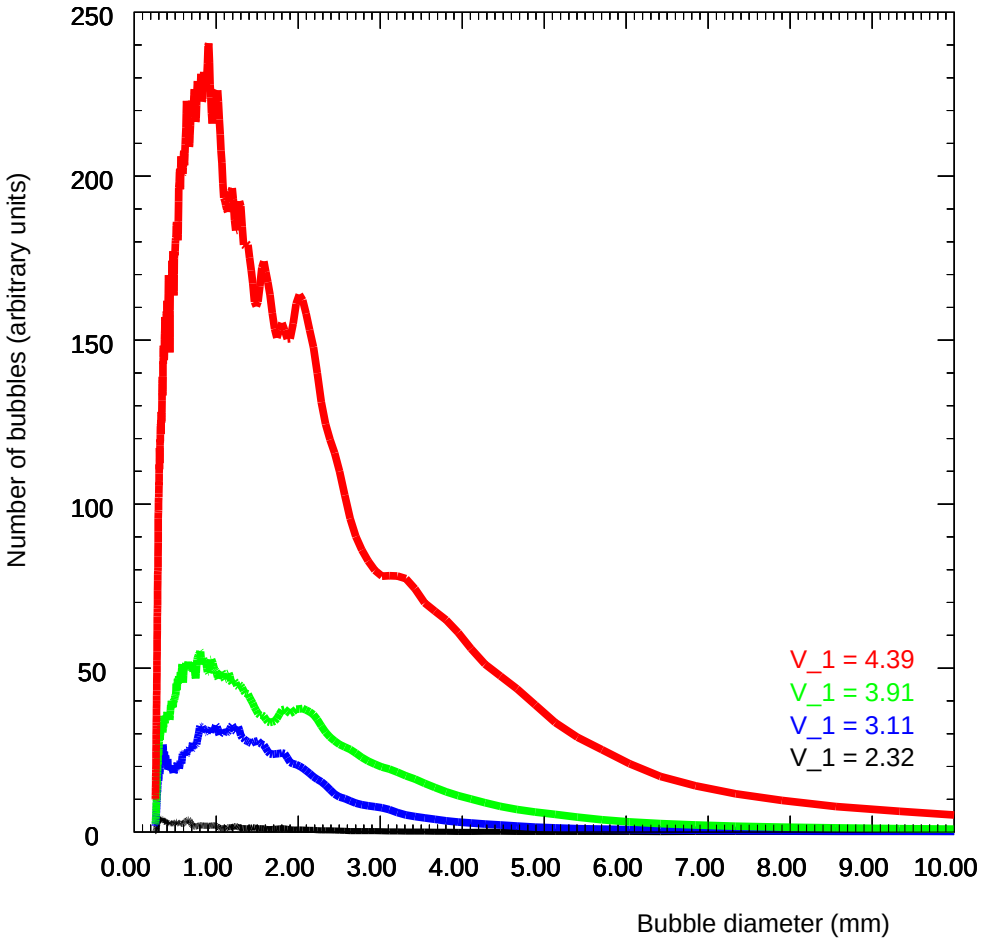

Figure 4. Bubble-size spectra, jet height 5 mm

the bubbles are excited both by their initial formation and by background turbulence, and it might be reasonable to assume ($R_0/\bar{R}$) being a constant. The overall factor K was assumed constant by Pandit et al. (1992) and in the present work. Fig. 4 presents bubble-size spectra for the acoustic data shown in Fig. 3. Note that the trends in raw frequency do not necessarily represent trends in bubble-size spectra.

For all acoustic experiments, the bubble size spectra show a peak in the production of bubbles around 1 mm in diameter. Resistivity-probe chord-length data for related two-dimensional flows also shows a peak around 1 mm (Cummings and Chanson 1997). The aliasing frequency of the equipment of 22 kHz implies a cut-off to bubbles below 0.3 mm in diameter. Since the peaks in Fig. 3 fall off well before 0.3 mm, it is believed that that they are genuine peaks, subject only the uncertainties of the assumptions detailed

above.

There is also a second peak around 2.0 mm diameter in both the $V_1 = 4.39$ m s^{-1} and $V_1 = 3.91$ m s^{-1} data and a peak at about 1.6 mm in the $V_1 = 4.39$ m s^{-1} data. The corresponding ratio 2.0/1.6 is about the cube root of two. It could be inferred that pairs of 1.6 mm bubbles are coalescing to form 2.0 mm bubbles, or alternatively that the 2.0 mm bubbles are breaking up (Cummings and Chanson 1998, 1999). However, Cummings and Chanson (1998) never observed bubble coalescence for $x - x_1 < 0.2$ m in a planar plunging jet, only breakup; both video and still photographs highlighted breakage.

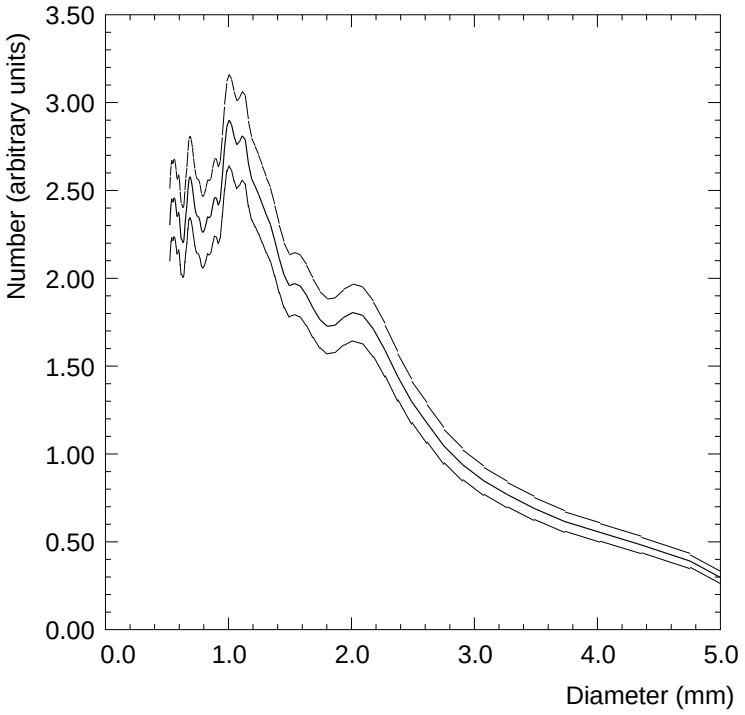

Figure 5. Detailed bubble size spectrum, jet height 5 mm, speed 3.9 m/s

The case of $V_1 = 3.91$ m s^{-1} corresponds to the resistivity probe data of Fig. 2(a). A detailed bubble size spectrum is shown in Fig. 5, in which as before the 95% statistical confidence interval is shown.

4.3. Bubble-size distributions

The Fourier-transform inversion method described above has a number of disadvantages (Manasseh et al. 2000); among these is the absence of data on bubble counts, which is readily provided by the resistivity probe. However, the alternative 'first-period' method detailed in Manasseh et al. (2000) yields a distribution of bubble sizes based on the identification of individual bubble pulses. These data can be used to infer bubble count rates as well as a size distribution. The method depends on an adjustable trigger

level which will tend to bias the results towards larger bubbles, equivalent to the bias in the spectrum-inversion approach above. Again, assumptions are required to correct the distribution. Following the reasoning in Manasseh et al. (2000), the use of a trigger means that only bubbles within a critical radius of the sensor get detected. This critical radius depends linearly on the bubble size. Therefore, assuming that the spatial distribution of bubbles is independent of their size, the number n of bubbles of a given size can adjusted to the true number N, by equalizing the critical volumes:

$$N = n(R_{0r}/R_0)^3, \tag{8}$$

where R_{0r} is any reference bubble radius. The distribution $N(R_0)$ is then normalized to ensure the total number of bubble counts is the same.

The bubble count rates derived from this method were very similar to the resistivity probe count (Fig. 2(a)), which peaks at about 10 counts per second. The similar cut-off size of 0.3 mm may have helped match the two techniques. The trigger level was fine-tuned to give a similar bubble count rate (4–5 counts/s) to the resistivity probe at the actual hydrophone location, and the corresponding distribution is shown in Fig. 6. Here, 1154 individual bubble pulses have been sorted into 166 bins, with the numbers adjusted following Eq. (8). If different trigger levels are chosen the distributions are similar. The distribution is consistent with the spectrum of Fig. 5, showing peaks around 1 mm and 1.5-2.0 mm diameter bubbles. However, more details are apparent, which may stem from the greater accuracy of the first-period method (Manasseh 1997). In particular, the peak around 1 mm is in fact a double peak with sub-peaks at 0.80 and 1.04 mm. Since the ratio of these sizes is close to the cube root of two, there may be a tendency for the 1.04 mm bubbles to split into two equal daughter bubbles. (Cummings and Chanson 1998, 1999).

5. Conclusions

Measurements in a circular plunging jet flow indicate that the spatial distribution of void fraction and bubble count rate is modelled by a solution of an advective diffusion equation. In the circular plunging jet, there is a spatial offset in the peak of void fraction and bubble count, as with other plunging jet flows (Brattberg and Chanson 1998).

Acoustic data, processed by two independent techniques, reveal a bubble size population with a maximum probability around 1 mm in diameter, consistent with resistivity probe data. Since the acoustic bubble size measurements are measurements of true bubble volume, their distributions can be used to infer the presence of bubble breakup or coalescence.

The acoustic technique can be accurately calibrated for individual bubbles precisely produced under laboratory conditions (Manasseh 1997). However, one issue is that it is difficult to assess its accuracy in complex, high void-fraction flows. This is due to the difficulty in making any comparative measurements using an alternative technique. The acoustic technique has so far yielded useful *relative* bubble size data, for example spatial differences in bubble size in a complex, high void-fraction flow (Manasseh et al. 2000).

The present results suggest that an acoustic technique calibrated through laboratory measurements can also yield useful, *absolute* data in high-void fraction flows. Moreover,

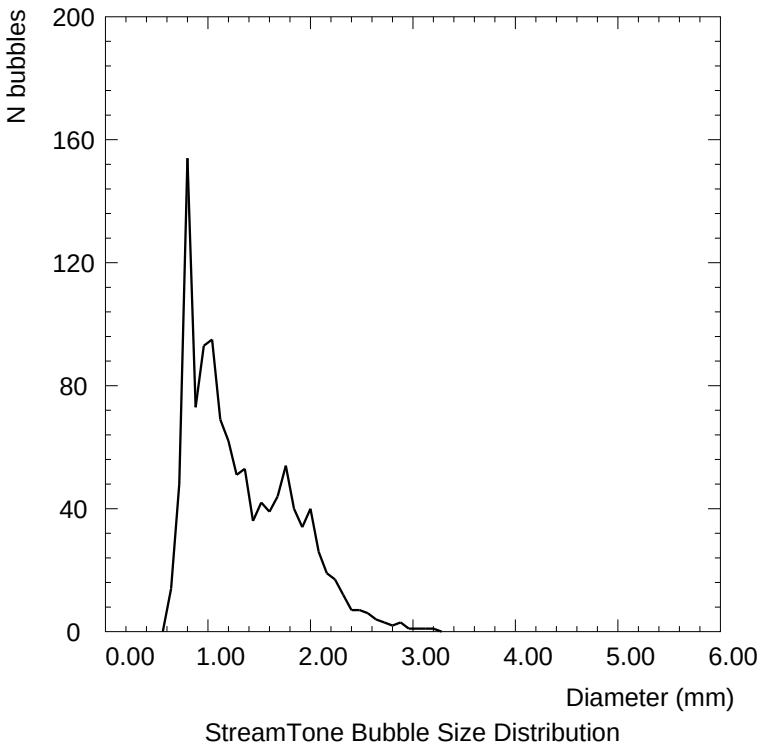

Figure 6. Bubble-size distribution, jet height 5 mm, speed 3.9 m/s

the robust acoustic sensor can then be used to make absolute measurements in hostile industrial or environmental flows where more delicate instruments are impractical.

References

Bin, A.K., 1993. Gas entrainment by plunging liquid jets. Chem. Eng. Sci., **48**(21), 3585–3630.

Chanson, H., 1997. Air bubble entrainment in free-surface turbulent shear flows. Academic Press, London, 401 pp.

Chanson, H. Brattberg, T., 1998. Air entrainment by two-dimensional plunging jets : the impingement region and the very-near flow field. Proc. 1998 ASME Fluids Eng. Conf., FEDSM'98, Washington DC, USA, June 21-25, Paper FEDSM98-4806, 8 pp.

Cummings, P. D., Chanson, H., 1997. Air entrainment in the developing flow region of plunging jets. Part 2 : Experimental. J. Fluids Eng., Trans. ASME **119**(3), 603–608

Cummings, P. D., Chanson, H., 1998. Individual air bubble entrapment at a planar plunging jet with near-inception flow conditions. Proceedings, 13th Australasian Fluid Mechanics Conference Monash University, Melbourne, Australia, 13–18 December 1998.

Cummings, P. D., Chanson, H., 1999. An experimental study of individual air bubble entrainment at a planar plunging jet. Chem. Eng. Research and Design, Trans. IChemE,

Part A, **77**(A2), 159–164.

Ervine, D. A., McKeogh, E. J., Elsawy, E. M., 1980. Effect of turbulence intensity on the rate of air entrainment by plunging water jets. Proc. Inst. Civil Eng., Part 2, June, 425–445.

Jameson, G.L., 1995. Bubbly flows and the plunging jet flotation column. Proc. 12th Australasian Fluid Mechanics Conference, Sydney, Australia, R.W. Bilger Ed. **2**, 735–742.

Kolani, A. R., Oğuz, H. N., Prosperetti, A., 1998. A new aeration device. Proc. 1998 ASME Fluids Eng. Summer Meeting, 21-25 June 1998, Washington, D.C., USA **257**, 111-145.

Leighton, T. G., 1994 The acoustic bubble. Academic Press, London.

Manasseh, R., 1997. Acoustic sizing of bubbles at moderate to high bubbling rates, Proc. 4th World Conference on Experimental Heat Transfer, Fluid Mechanics and Thermodynamics, Brussels, 2–6 June 1997.

Manasseh, R., LaFontaine, R. F., Davy, J., Shepherd, I. C., Zhu,Y., 2000. Passive acoustic bubble sizing in sparged systems. Experiments in Fluids (in press).

Minnaert, M., 1933. On musical air bubbles and the sound of running water. Phil. Mag., **16**, 235–248.

Pandit, A. B., Varley, J., Thorpe, R. B., Davidson, J. F., 1992. Measurement of bubble size distribution: an acoustic technique. Chem. Eng. Sci. **47**(5), 1079–1089.